

ON TWO SCHEMES FOR NUCLEAR REACTOR CALCULATIONS.

=====

R. Ortiz, G. Velarde, R. Caro, J.L. de Francisco and A. Brú<sup>(\*)</sup>

Junta de Energía Nuclear, Madrid.

1.- Calculation of few-group constants

According to the first scheme, few-group nuclear constants are generated by averaging over a given spectrum, either a moderation spectrum or a thermal spectrum.

1.1.- Fast constants.

The energy interval 0.625 eV - 10 MeV is divided into a number of  $g$  energy groups, with  $g \leq 3$ . The group constants are averages over the flux spectrum,  $F_0(u)$ , obtained as the solution of the Boltzmann equation for an infinite, homogeneous slab in the  $P_1$  or  $B_1$  approximation. The external source is supposed to be isotropic. The slowing-down density,  $q$ , for hydrogen is the solution of

$$\frac{dq}{du} + q = \sum_s F_0 \quad (1)$$

(\*) Including work by T. Iglesias, F. Briones, and M.R. Corella

All other components of  $q$  for non-hydrogenous elements are computed by the approximation

$$q_j = (\lambda \cdot \Sigma_a + \xi \Sigma_s) \cdot F_0 \quad (2)$$

where  $\lambda = \bar{\xi}^2 / 2 \xi$ . Although a new version of the program ISLERO allows to handle deuterium according to the consistent Greuling-Goertzel approximation, the calculations performed were all based on Eq. (2), except for hydrogen, and the  $B_1$  approximation.

The slowing-down equations are solved by the programs ISLERO-0, and ISLERO-1 [1]. ISLERO-0 gives the average macroscopic constants; ISLERO-1 provides both the few-group macroscopic and microscopic constants for each element. Input data are: atomic densities,  $N_i$ , of the different elements, buckling - either constant or group depending in ISLERO-1 - and self-shielding factors,  $L$ , for each element which exhibits resonances. An average  $L$  factor, as well as  $\nu_{t}^{25}$ , may be introduced as an adjustable parameter for each reactor type. In the case of the DON reactor (19 rod elements of UC, with Al and SAP as structural materials, organic cooled,  $D_2O$  moderated reactor) no adjustment was made in the preliminary stage of the calculations. For  $\nu_{t}^{25}$  the value 2'43 was adopted [18] and the average  $L$  value was computed according to a formula given in [2]. The effective resonance integral was assumed to be given by

$$IR_r = IR_0 \left[ 1 + (a+b) \frac{S_{ef}}{M} \left( \sqrt{T^{comb}} - 17'1348 \right) \right] \quad (3)$$

where

$$IR_o = A + B \sqrt{\frac{S_{ef}}{M} + E} \quad (4)$$

and

$$S_{ef} = S_g (1 - C) \quad (5)$$

$S_g$  is the (geometric) surface area of the absorbing elements, and  $C$  the Dancoff-Ginsburg coefficient

$$C = \frac{2}{\pi L'} \int dL' \int \cos \beta \cdot K_{i3} (\Sigma_s \lambda) \cdot d\beta \quad (6)$$

where  $\lambda$  is the chord-length in the moderator between two points on the fuel,  $\beta$  the angle with the outward directed normal to the fuel surface and  $L'$  the element of length on the fuel surface normal to the axis.

Values for the parameters  $A, B, E, a,$  and  $b$  are given in Table I. As for the UC, use was made of the Vernon correlation formulae [3] for  $UO_2$  and  $U$ . The following intermediate formula obtains [4]:

$$IR_o^{uc} = 3'64 + 25'87 \sqrt{\left(\frac{S_{ef}}{M}\right)^{uc}} \quad (7)$$

Values of  $C$  for two rods have been given by Carlvik and Pershagen [6]. For rod bundles, the correction proposed by Fukai [7] has been taken into account. Velarde has computed  $C$  values, for infinitely long cylindrical rings [8].

## 1.2.- Thermal constants.

The thermal region limits are 0 and 0.625 eV. There is only one thermal group (cf., 2), and the corresponding constants are averages over a thermal flux spectrum. The thermal spectrum results from the integration of an elementary form of the neutron transport equation under the following simplifying assumptions: a) thermalization takes place in an infinite, homogeneous, isotropic medium, neutron leakage being represented by a  $DB^2$  term in practical cases; b) the scatterer is a monoatomic gas; c) the mass of the scattering nuclei is: i) either equal to or much greater than the neutron mass through the interval 0 - 0,625 eV (Wigner-Wilkins and Wilkins spectrum, respectively); ii) much greater than the neutron mass in an interval  $0 < E < E_c$  and equal to the neutron mass in the interval  $E_c \leq E < E_0 = 0,625$  eV. Under these conditions, the problem reduces to the integration of an ordinary differential equation of the form

$$y''(E) = -H(E) \cdot y(E) \quad (8)$$

where  $H(E)$  is a continuous function of  $E$  in the interval  $(0, E_0)$  in the first case, and has an ordinary discontinuity at  $E_c$  in the second case. The solution looked for,  $y(E)$ , is that solution which is continuous, together with its first derivative, in the interval  $(0, E_0)$  and is zero for  $E = 0$ . As a consequence, the neutron density  $N(E)$  is continuous in  $(0, E_0)$ , but its first derivative has an ordinary discontinuity at  $E_c$  if  $H(E)$

is discontinuous at  $E_c$ . The programs PROMETEO-1, PROMETEO-2 and PROMETEO-3 [9, 10, 11] solve the differential equation (8) and give the corresponding flux spectrum,  $F_0(E)$ , for the three cases Wigner-Wilkins, Wilkins, and Wilkins ( $0 < E < E_c$ ) - Wigner-Wilkins ( $E_c \leq E < E_0$ ), respectively. Input parameters are: atomic densities for each material; buckling; moderator temperature; an index characterizing the effects of chemical binding.

### 1.3.- Void regions.

Practically void regions, such as a coolant annulus of a gas of very small cross-sections or a gaseous thermal insulator, may be treated as a purely scattering medium in multigroup diffusion theory. For a cylindrical layer the void region multigroup constants are all zero but the diffusion coefficient,  $D^V$ , which is given by [12]

$$D^V = \frac{r_{v-1}}{2\alpha} \cdot \text{Log} \frac{r_v}{r_{v-1}} \approx 1 \pm 0.2 \quad \text{for } 0.15 \leq \frac{r_{v-1}}{r_v} \leq 0.85 \quad (9)$$

where

$$\alpha = 1 - \frac{2}{R} \arcsin \frac{r_{v-1}}{r_v} - \frac{2}{R} \cdot \frac{r_{v-1}}{r_v} \left( 1 - \frac{r_{v-1}}{r_v} \right)^{\frac{1}{2}}$$

and  $r_v$ ,  $r_{v-1}$  are the external and the internal radii of the layer.

### 1.4.- Fine structure.

The heterogeneities of the fuel region, with the fuel slugs, the cladding and the organic liquid have been taken into account as follows. For the resonance group, the effective surface  $S_{\text{eff}}$  takes care of the inhomogeneity of the system. For the thermal group, disadvantage factors can be -

computed from one-velocity diffusion theory, as applied to the coolant, and from multiple collisions for the cladding and fuel. The extrapolation length allows the matching of the two models through the equation

$$\lambda \cdot \sum_{tr}^r = \frac{4}{3\beta} - H \quad (10)$$

where  $\sum_{tr}^r$  refers to the coolant and  $H = 4r^c \cdot \sum_{tr}^r \cdot J^{in}$ .  $r^c$  is the cladding radius,  $J^{in}$  = input current on the cladding surface due to the neutron flux in an infinite medium without capture [13], and  $\beta$  is the blackness of cladding and fuel [13, 14]. A better estimate for  $H$  follows from the extrapolation length  $\lambda_{neg}$  for a black rod, either measured, or computed by means of more detailed models. From  $\beta = 1$  follows  $H = \frac{4}{3} - \lambda_{neg} \cdot \sum_{tr}^r$ . This was the method adopted, with the simplifications proposed by Pershagen and Carlvik [14].

## 2.- Cell integral parameters.

With the fast and thermal values of the constants for the  $g \leq 4$  energy groups, and for each homogenized region of the cell, as well as with the effective diffusion coefficient (Eq.9) corresponding to the void regions, the diffusion equations are solved for the  $g$  components of the flux, and the infinite multiplication factor,  $k$ , and the cell material buckling computed. By suitably dividing the cell into

regions, and by properly homogenizing these regions, it is possible to apply the few groups diffusion model as a first approximation. As is well known, a more precise treatment - will be needed in many cases. But although we are well aware that the method we have allowed is rather crude for cell calculations, nevertheless the programs EDIPO-1 and EDIPO-2 [15] were used to compute cell integral parameters. EDIPO-1 solves the one-dimensional, multigroup diffusion equations

$$\begin{aligned} \nabla D_i \nabla \phi_i - \left[ D_i B_{i,i}^2 + \Sigma_{a,i} + \sum_{j=i+1}^g \Sigma_{i \rightarrow j} \right] \phi_i + \\ + \sum_{j=1}^{i-1} \Sigma_{j \rightarrow i} \phi_j + \frac{1}{\lambda} \chi_i \sum_{j=1}^g (v \Sigma_f)_j \phi_j = 0 \end{aligned} \quad (11)$$

for  $g \leq 4$  energy groups, and a maximum of 20 regions and 199 mesh points. The results are the components of the flux and the eigenvalue  $k_\infty = \lambda$ . The material buckling,  $B_m$ , is computed as the largest root of the secular equation associated to Eq. (11), with  $\lambda = 1$ , [16]. EDIPO-2 solves essentially the same problem Eq. (11), with  $g \leq 16$ , for a maximum of 5 regions and 49 mesh points. The main difference is in that EDIPO-2 allows for up-scattering in the last three groups, and 3 effective thermal groups, which are treated following essentially the Selengut scheme.

## 2.1.- Iteration process.

As said before, the volume averaged atomic densities are taken as input data to evaluate the few group cons-

tants in the first iteration. The foregoing procedure allows then to compute the distributions of the  $g$  flux components throughout the cell. The next step consists in a new evaluation of the few group constants, with the atomic densities weighted according to the product flux  $\times$  volume. The iteration process is repeated until the values for the infinite multiplication constant or the material buckling in succeeding iterations coincide according to a given convergence criterion. For survey purposes in connexion with optimization calculations, the first iteration is usually acceptable.

### 3.- Synthesis method.

The UNIVAC USS-90 computer is not large enough to handle two-dimensional, multigroup diffusion problems, either because of capacity requirement and / or the very large amounts of computer time involved. Because of this a program has been prepared to construct synthesized two-dimensional fluxes from the results of one-dimensional calculations [17]. The method is essentially the so called "conventional" synthesis method. Let  $i = 1, 2, \dots, n$  be the axial zone index, and  $\mu = 1, 2, \dots, g$  the energy group index. A transverse calculation with EDIPO-1 gives the (in general, non-normalized) solution of

$$\begin{aligned} \operatorname{div}_x D_\mu \operatorname{grad}_x \varphi_\mu^i(x) - \left\{ \Sigma_{T\mu} + D_\mu B_{z\mu}^2(\mu) \right\} \varphi_\mu^i(x) + \\ + \sum_{\nu=1}^{M-1} \Sigma_{\nu\mu} \varphi_\nu^i(x) + \frac{1}{\lambda_x} \chi_\mu \sum_{\nu=1}^g (\nu \Sigma_F)_\nu \phi_\nu^i(x) = 0 \end{aligned} \quad (12)$$



satisfying suitable boundary conditions, and the corresponding eigenvalue  $\lambda_x(i)$ . Of course at the outset of a calculation first estimates for the axial bucklings  $B_{z\mu}^2(i)$  have to be introduced in Eq. (12) for each axial zone. Once the fluxes are obtained, an axial calculation is performed by solving the equation

$$\begin{aligned} \bar{D}_\mu^i z_\mu''(z) - \left( \bar{\Sigma}_{T\mu}^i + \bar{D}_\mu^i B_{x\mu}^2(i) \right) z_\mu(z) + \\ + \sum_{\nu=1}^{\mu-1} \bar{\Sigma}_{\nu\mu}^i z_\nu + \frac{1}{\lambda_x} \sum_{\nu=1}^3 \overline{\chi_{\mu(\nu \xi_F)}^i} z_\nu = 0 \end{aligned} \quad (13)$$

for the solution subject to appropriate boundary conditions, and the corresponding eigenvalue. In Eq. (13) the averages are defined by

$$\bar{f}_\mu^i = \frac{\int_{(z)} dx f_\mu(x) \varphi_\mu^i(x)}{\int_{(z)} dx \varphi_\mu^i(x)} \quad (14)$$

and

$$\begin{aligned} \bar{D}_\mu^i B_{x\mu}^2(i) \int_{(z)} \varphi_\mu^i(x) dx = \\ = \sum_{\nu=1}^3 \left[ \bar{\Sigma}_{\nu\mu}^i + \frac{1}{\lambda_x} \overline{\chi_{\mu(\nu \xi_F)}^i} \right] \int_{(z)} \varphi_\nu^i dx + \left[ \bar{\Sigma}_{T\mu}^i + \bar{D}_\mu^i B_{z\mu}^2(i) \right] \int_{(z)} \varphi_\mu^i dx \end{aligned} \quad (15)$$

From the solution  $z_\mu(z)$  and  $\lambda_2$  of (13), a new series of  $n$  transverse calculations is started according to Eq. (12), and with the axial bucklings given by

$$\bar{D}_\mu^i B_{2\mu}^2(i) \int_{z_{i-1}}^{z_i} z_\mu(z) dz = \sum_{\nu=i}^3 \left[ \bar{\Sigma}_{\nu\mu}^i + \frac{1}{\lambda_2} \overline{\chi_{\mu}(\nu z_{\nu})}^i \right] \int_{z_{i-1}}^{z_i} z_\nu dz - \left[ \bar{\Sigma}_{T\mu}^i + \bar{D}_\mu^i B_{x\mu}^2(i) \right] \int_{z_{i-1}}^{z_i} z_\mu dz \quad (16)$$

This process is repeated until the values  $\lambda_1$  and  $\lambda_2$  coincide to the desired accuracy. The convergence rate used to be satisfactory.

#### 4.- Experiments on AQUILON-II and at J.E.N.

The foregoing mathematical scheme has been tested against the results of exponential experiments carried out at the Physics Division of J.E.N., and some substitution experiments on AQUILON-II. The cell used is of the 20 type for the DON reactor (Fig. 1). The exponential experiments have been performed on the complete cell, with calandria, process and shroud tubes, whereas the substitution measurements were performed on two UC lattices, 20S and 20E.

The fuel elements for the 20S lattice are the same as in Fig. (1), but without tubes for organic. The fuel assemblies for the 20E lattice are as shown in Fig. (1), that is, with organic liquid and the 19 UC slugs housed in the shroud tube. The fuel assemblies were always on a square lattice, with lattice pitch equal to 19, 21, and 24 cm. The

AQUILON-II aluminum vessel [19] (0,6 cm. thick at the side wall, and 1 cm. thick at the bottom) houses the 112 fuel assemblies of  $UO_2$  in  $D_2O$  constituting the reference assembly. 4, 12, 16, and 24 UC test fuel assemblies are substituted, successively, for reference fuel assemblies in central positions. Between the reference lattice and the vessel walls there is left a  $D_2O$  reflector. The lateral graphite reflector, surrounding the cylindrical aluminum vessel, is in the form of a hollow octogonal prism (apothem length = 205m), 2,90 m interior diameter. The system vessel-graphite is on a graphite block, 0,70 m. high. The reference fuel assemblies are composed of 7  $UO_2$ , aluminum clad rods, 22 mm in diameter, on a centered hexagon. The cladding to cladding spacing is equal to 7 mm.

Table II shows the computed as well as the measured values for the material buckling, and Figs. 2 and 3 give the computed values for  $k_{\infty}$  also.

AQUILON-II was brought to criticality for every tested configuration. As a result, we had at our disposal a set of critical systems that allowed us to test the mathematical scheme by computing the corresponding set of  $k_{eff}$  values and comparing them with unity. Given the elementary character of the scheme, the results were expected to be rather rough. But it was decided to perform the calculation in order to assess afterwards the relative merits of the different approximations. The geometrical model is shown in Fig. 4, and the dimension are given in Table III. The results arrived at are shown in Tables IV and V.

## 5.- Statics of fast reactors.

### 5.1.- Calculation of constants.

The mathematical tools of the model are ~~two~~ programs, CAMPEADOR and EDIPO, both within the multigroup ~~diffu~~ diffusion approximation. The program CAMPEADOR solves the multi-group diffusion equations for a finite, homogeneous medium. The nuclear constants are those of the sixteen group set compiled by Yiftah, Okrent and Moldauer [21]. The sixteen flux components are computed as solution of the system of equations

$$\begin{aligned}
 -D_i B_i^2 \phi_i - \Sigma_{a_i} \phi_i - \sum_{j=i+1}^{16} \Sigma_{i \rightarrow j} \phi_j + \\
 + \sum_{k=1}^{i-1} \Sigma_{k \rightarrow i} \phi_k + \frac{\lambda_i}{k_{eff}} \sum_{\gamma=1}^{16} (\nu \Sigma_f)_{\gamma} \phi_{\gamma} = 0
 \end{aligned} \tag{18}$$

The sixteen importance components are the solution of the adjoint system

$$\begin{aligned}
 -D_i B_i^2 \phi_i^{\dagger} - \Sigma_{a_i} \phi_i^{\dagger} - \sum_{j=i+1}^{16} \Sigma_{i \rightarrow j} \phi_j^{\dagger} + \\
 + \sum_{j=i+1}^{16} \Sigma_{i \rightarrow j} \phi_j^{\dagger} + \frac{\nu \Sigma_{f_i}}{k_{eff}} \sum_{j=1}^{16} \lambda_j \phi_j^{\dagger} = 0
 \end{aligned} \tag{19}$$

Both systems are reduced to the triangular form by setting

$$\frac{1}{k_{eff}} \sum_{\gamma=1}^{16} (\nu \Sigma_f)_{\gamma} \phi_{\gamma} = 1 \quad \text{in Eq. (18), and} \quad \frac{1}{k_{eff}} \sum_{j=1}^{16} \lambda_j \phi_j^{\dagger} = 1$$

in Eq. (19),

From either the solution of (18), or the solutions of (18) and (19), CAMPEADOR averages the nuclear constants to arrive at a set of  $g \leq 16$  constants, either by averaging over the flux spectrum, or over the spectrum of the product  $\phi^{\dagger} \cdot \phi$ . The program allows to compute the effective multiplication factor,  $k_{eff}$  for bare systems ac-

according to the formula

$$k_{eff} = \frac{\sum_{r=1}^{16} (\nu \Sigma_f)_r \phi_r}{\sum_{r=1}^{16} (D_r B^2 + \Sigma_{ar}) \phi_r} \quad (20)$$

as well as the material buckling by iteration until  $k_{eff} = 1$ . The infinite multiplication value is obtained by setting  $B^2=0$  in Eq. (18) or (19).

To study small and highly concentrated bare systems, the program offers as an alternative to the diffusion leakage term  $B^2 / 3\Sigma_{tr}$  the use of the corresponding value for the asymptotic solution of the transport equation  $\frac{B^2}{\text{arbitrary } \Sigma_{tr}} - \Sigma_{tr}$ . The second representation leads to a better description of the flux, and to better values for the critical masses.

## 5.2.- Tests of the calculation scheme.

The calculation scheme has been tested by comparison with experimental results from studies on two highly concentrated, bare fast neutron systems (Godiva and Jezebel, [23]), and on four reflected ZPR-III configurations [24,25]. The critical masses for Godiva and Jezebel were computed according to diffusion theory. As expected, the values arrived at when leakage is represented by a term  $B^2 / 3\Sigma_{tr}$  are considerably greater than the experimental values. By estimating leakage as follows from the asymptotic solution of the Boltzmann equation, the computed critical masses are in better agreement with experiment, though they are smaller than the actual values. The results are shown in Table VI. As to the four fast reactor confi-

gurations in EPR-III, the 16 group set of constants was reduced to 4 energy group following two averaging processes, as explained above. The buckling in Eqs. (18) and (19) was supposed group independent and equal to the material buckling. Reactivity and flux distributions are then computed with the EDIPO program and the conventional synthesis method as described in 2 and 3. In some cases, a group depending buckling is deduced from the computed flux distributions, and new constant averages are performed with CAMPBADOR to arrive at a new set of four energy group constants, from which a new reactivity value follows with EDIPO.

The results are given in Table VI. Column A(B) shows the values which have resulted from the first (second) average procedure.

. - . - .

The results shown in Tables IV and V have to be considered insufficient to provide a good estimate of the critical mass. Some improvements might result from succeeding iterations for the cell constants, and, perhaps, from parameter adjustments and or model modifications. On the other hand, Tables VI and VII seem indicate a similar situation. There is the possibility of improving it by iteration. But the comparison between theory and experiment becomes particularly involved in this case because of the difficulties of correctly taking into account the inhomogeneity effects in a rather crude model.

ACKNOWLEDGEMENTS.

The authors wish to express their thanks to Atomic International for their assistance in the calculation of the fast constants for the fuel elements designed for the DOE Reactor Project.

TABLE IParameters for the resonance integrals.

Isotope	Metal	UO <sub>2</sub>		UC	
A	2,95	4,15	4,15	2,81	3,64
B	25,80	26,60	25,60	25,315	25,87
E	0	0	-0,02795	0,04529	0
a x 10 <sup>2</sup>	0,51	0,58	0,55	0,55	0,55
b x 10 <sup>2</sup>	0,50	0,50	0,50	0,50	0,50
Reference.	/5/	/5/	/4/	/4/	/4/



T A B L E II

Computed vs. measured  
material bucklings.

CELL	CELL SPACING		D <sub>2</sub> O PURITY, %	B <sup>2</sup> <sub>m</sub> , m <sup>-2</sup>		
	hexagonal lattice	square lattice		COMPUTED	MEASURED	
					Exp. JEN	Aguillon II <sup>2</sup>
20 F	21,59	20,092	99,75	1,23	1,44 $\pm$ 0,09	
	24,13	22,456	99,75	1,65	2,04 $\pm$ 0,09	
	26,67	24,819	99,75	2,02	2,25 $\pm$ 0,08	
20 E	20,417	19	99,50	3,74		4'08
	22,566	21	99,50	4,11		4'22
	25,789	24	99,50	3,98		3'94
20 S	20,417	19	99,50	5,11		5'44
	22,566	21	99,50	5,64		5'84
	25,789	24	99,50	5,52		5'55
FOEL'7	20,417	19	99,50	5,24		
	22,567	21	99,50	5,44		
	25,789	24	99,20	5,13		
DT-UO <sub>2</sub>	26,67	24,819	99,75	1,05	1,25 $\pm$ 0,08	

According to J.L. de Francisco /20/.

TABLE III .:

Dimensions of the geometrical modelRadial dimensions20-S and 20-E lattices

Lattice spacing	OR <sub>0</sub> (Number of substituted elements)					OR <sub>1</sub>	OR <sub>2</sub>	OR <sub>3</sub>	OR <sub>4</sub>
	0	4	12	16	24				
19	0	21'43	37'13	42'08	52'54	113'45	145	145'6	211'95
21	0	23'69	41'03	47'40	56'04	125'39	"	"	"
24	0	27'07	46'90	54'17	66'34	143'30	"	"	"

Axial dimensions.

S CELL

Lattice spacing	OR <sub>1</sub> (Number of substituted elements)					H <sub>1</sub> H <sub>2</sub>	H <sub>2</sub> H <sub>3</sub>	H <sub>3</sub> H <sub>4</sub>
	0	4	12	16	24			
19	148'80	148'38	147'97	147'97	147'44	7'5	1	71'95
21	141'44	140'81	139'41	138'94	137'87	"	"	"
24	147'45	146'36	144'31	143'52	141'99	"	"	"

E CELL

Lattice spacing	OR <sub>1</sub> Number of substituted elements					H <sub>0</sub> H <sub>1</sub>	H <sub>1</sub> H <sub>2</sub>	H <sub>2</sub> H <sub>3</sub>	H <sub>3</sub> H <sub>4</sub>
	0	4	12	10	24				
	OH <sub>1</sub> =148'74	OH <sub>1</sub> =151'92	7'74	11'46	19'16	151	7'5	1	71'95
	OH <sub>1</sub> =141'96	OH <sub>1</sub> =144'88	OH <sub>1</sub> =150'8	3'06	9'76	"	"	"	"
	OH <sub>1</sub> =147'71	OH <sub>1</sub> =151'31	7'85	11'58	20'12	"	"	"	"

TABLE IV

Computed values for  $k_{off}$ , 20-S cell experiments.

Number of substituted elements	Pitch 19	Pitch 21	Pitch 24
0	0,991	0,995	1,000
4	0,990	0,994	0,999
12	0,989	0,993	0,998
16	0,989	0,993	0,998
24	0,988	0,993	0,998

TABLE V

Computed values for  $k_{off}$ , 20-E cell experiments.

Number of substituted elements	Pitch 19	Pitch 19	Pitch 24
0	0,991	0,995	1,000
4	0,991	0,994	1,000
12	0,991	0,995	1,001
16	0,992	0,995	1,002
24	0,992	0,998	1,003

TABLE VI.

Critical masses (kg of fuel, U-235, Pu-239),  
of highly concentrated, bare systems

System	Ref.	Diffusion leakage	Transport leakage	Experiment	Geometry
Godiva	3	63,5	41,1	48,7	esfera.
Jezebel	3	29,7	12,5	16,22	esfera.

TABLE VII

Computed  $k_{eff}$  for ZPR-III critical assemblies

System	Ref.	Geometry	A	B
6 C	/24/	cylinder	0,956	0,976
6 F	/24/	sphere	1,011	1,011
9	/24/	cylinder	1,010	1,009
9 A	/24/	sphere	1,004	1,007

REFERENCIAS

- /1/ F. Briones.  
PTCR 4, Julio 1961 (Informe interno J.E.N.)
- /2/ G. Velarde.  
PTCR 24, Enero 1964 (Informe interno J.E.N.)
- /3/ R. Vernon.  
Nuc. Sc. Eng., 6, 163, Agosto 1959
- /4/ G. Velarde.  
PTCR 23, Enero 1964 (Informe interno J.E.N.)
- /5/ E. Hellstrand et al.  
Nuc. Sc. Eng. 8, 497, 1960.
- /6/ I. Carlvik, B. Pershagen.  
RFR 20, Febrero 1959
- /7/ Y. Fukai.  
Nuc. Sc. Eng. 9, 370, 1961
- /8/ G. Velarde.  
Nuc. Sc. Eng. 15, 1, 99, 1963.
- /9/ M. R. Corella, T. Iglesias,  
"Prometeo I", programa para promediar las constantes  
térmicas con un espectro de Wigner-Wilkins. (in press)

- /10/ M. R. Corella, T. Iglesias.  
"Prometeo II", programa para promediar las constantes  
térmicas con un espectro Wilkins. (In press)
- /11/ M. R. Corella, T. Iglesias.  
"Prometeo III", programa para promediar las constantes  
térmicas con los espectros Wilkins y Wigner-Wilkins.  
(In press).
- /12/ G. Velarde.  
Nuc. Sc. Eng. 13, 2, 200 (1962).
- /13/ C. D. McKay.  
NEI 143, Junio 1960.
- /14/ B. Pershagen, I. Carlvik.  
AEP 69.
- /15/ T. Iglesias.  
FTCR 13, Marzo 1963 (Informe interno J.E.N.)
- /16/ A. Brú.  
FTCR 30, (Informe Interno J.E.N.)
- /17/ R. Ortiz Fornaguera y T. Iglesias.  
FTCR 32, Marzo 1964 (Informe interno J.E.N.)
- /18/ ANL - 5800, Second Edition
- /19/ Bailly et col.  
DEP/EC/S 60-52 Juin 1960.

- /20/ E. Rodriguez Mayquez, J.L. De Francisco, F. Olarte.  
A/ Conf 28/A/ 1964.
- /21/ S. Yiftah et al.  
Fast Reactor Cross sections.  
Pergamon Press.
- /22/ R. Caro.  
CAMPEADOR, A condensation code for fast reactors.  
EAES Symposium on Fast and Epithermal Spectra in  
Reactors. Harwell, December 1963.
- /23/ W. B. Lowenstein and D. Okrent.  
P/637 2<sup>a</sup> Conferencia de Ginebra.
- /24/ J. K. Long et al.  
P/598 2<sup>a</sup> Conferencia de Ginebra.
- /25/ J. K. Long et al.  
Experimental Results on large dilute fast critical  
systems with metallic and ceramic fuels. Proceedings  
of the seminar on the physics on fast and interme-  
diate reactors.  
IAEA. Vol. I. Vienna.

LIST OF FIGURES

Fig. 1

DON CELL 20T

Fig. 2

DON CELLS 20E and 20S,  $K_{\omega}$  and  $B_m^2$

Fig. 3

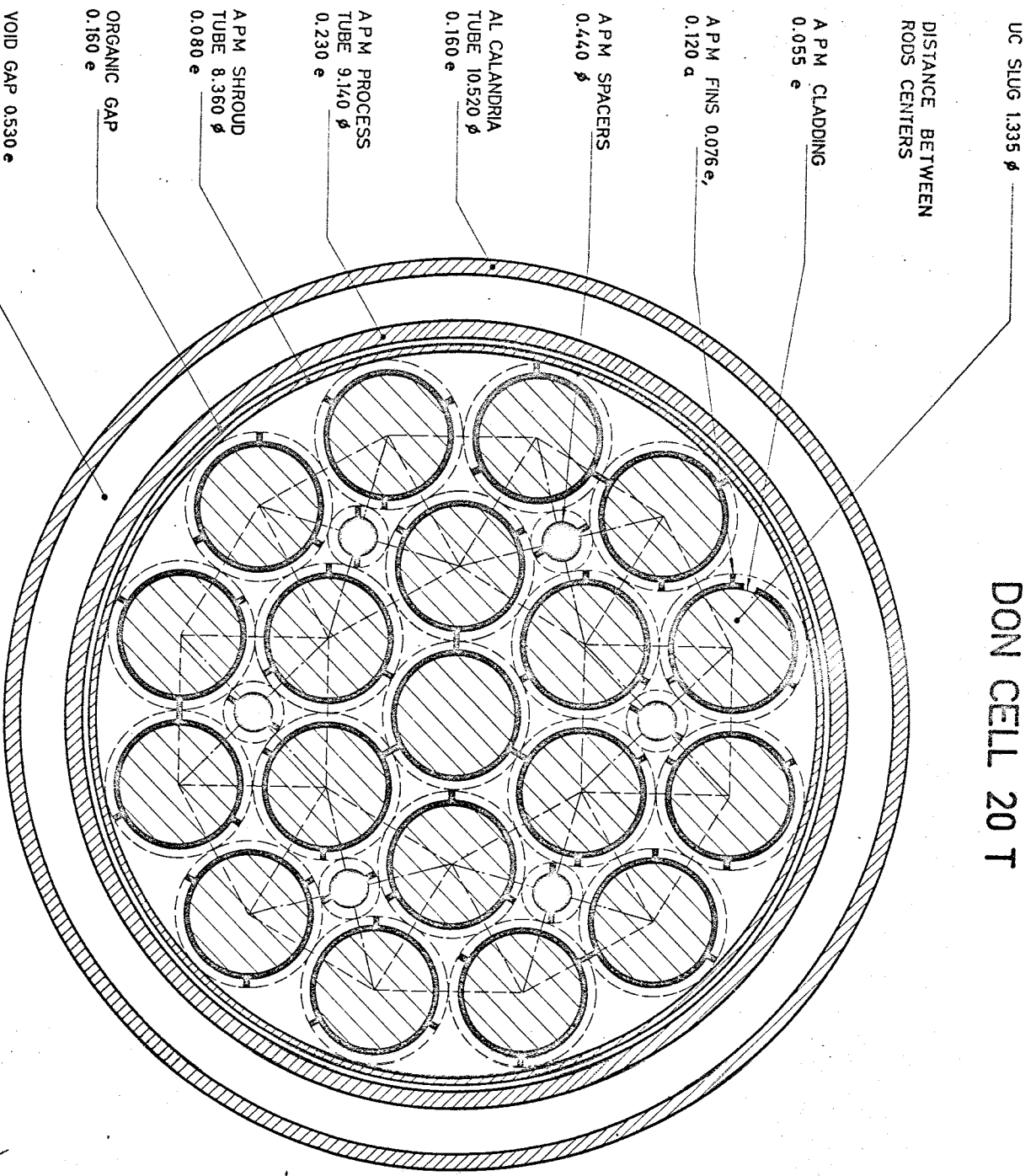
DON CELLS 20T and 20T -  $UO_2$ ,  $K_{\omega}$  and  $B_m^2$

Fig. 4

GEOMETRICAL MODEL



# DON CELL 20 T



UC SLUG 1.335  $\phi$

DISTANCE BETWEEN  
RODS CENTERS

A P M CLADDING  
0.055 e

A P M FINNINGS  
0.120 a

A P M SPACERS  
0.440  $\phi$

AL CALANDRIA  
TUBE 10.520  $\phi$   
0.160 e

A P M PROCESS  
TUBE 9.140  $\phi$   
0.230 e

A P M SHROUD  
TUBE 8.360  $\phi$   
0.080 e

ORGANIC GAP  
0.160 e

VOID GAP 0.530 e

CELL 20T-UO<sub>2</sub> — the same as  
20 T but with  
UO<sub>2</sub>

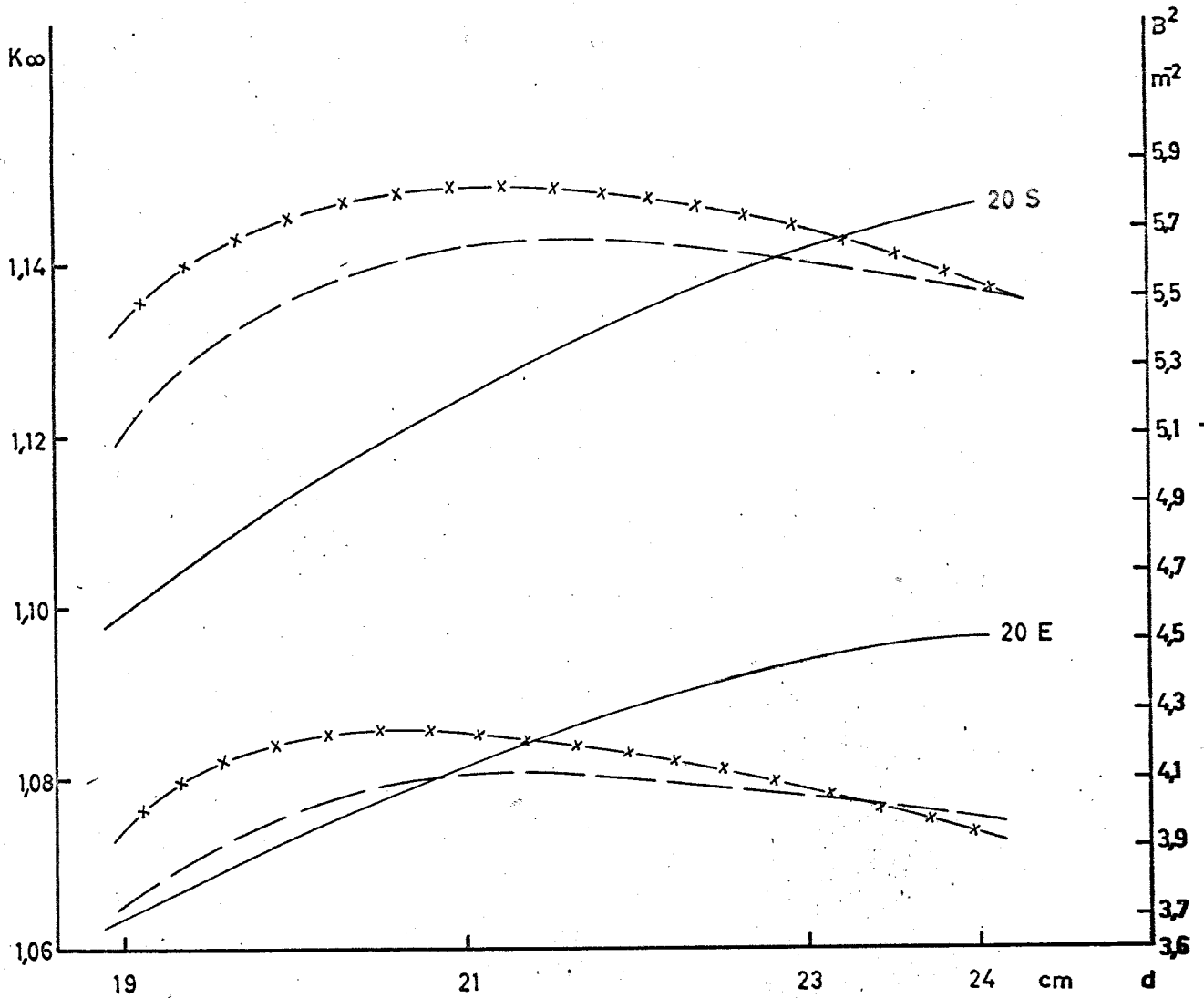
CELL 20 E — the same as  
20 T but without  
process and  
calandria tubes,  
and without  
organic and void  
gaps.

CELL 20 S — the 19 UC slugs  
in D<sub>2</sub>O

SCALE 2:1  
in cm  
 $\phi$  = outer dia.  
e = thickness  
a = height

Fig. 1

DON CELLS 20E AND 20S  
 $K_{\infty}, B^2$



$K_{\infty}$  —————  
 $B^2$  - - - - - Calculated.  
 $B^2$  -x-x-x-x- Measured in Aquilon II (Saclay) and interpreted by De Francisco

Fig. 2

DON CELLS 20 T AND 20T-UO<sub>2</sub>  
 $K_{\infty}, B^2$

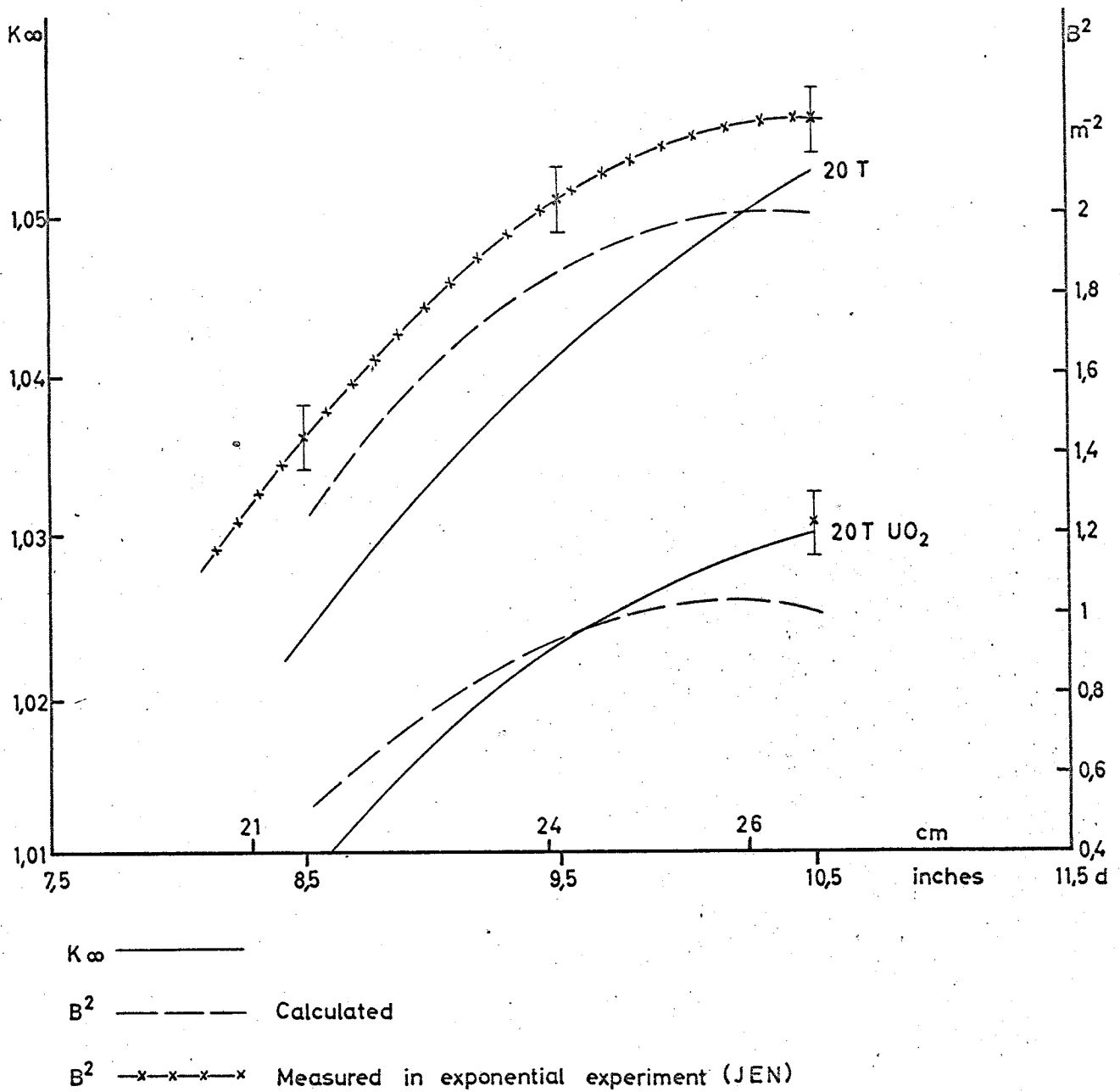


Fig. 3

# GEOMETRICAL MODEL

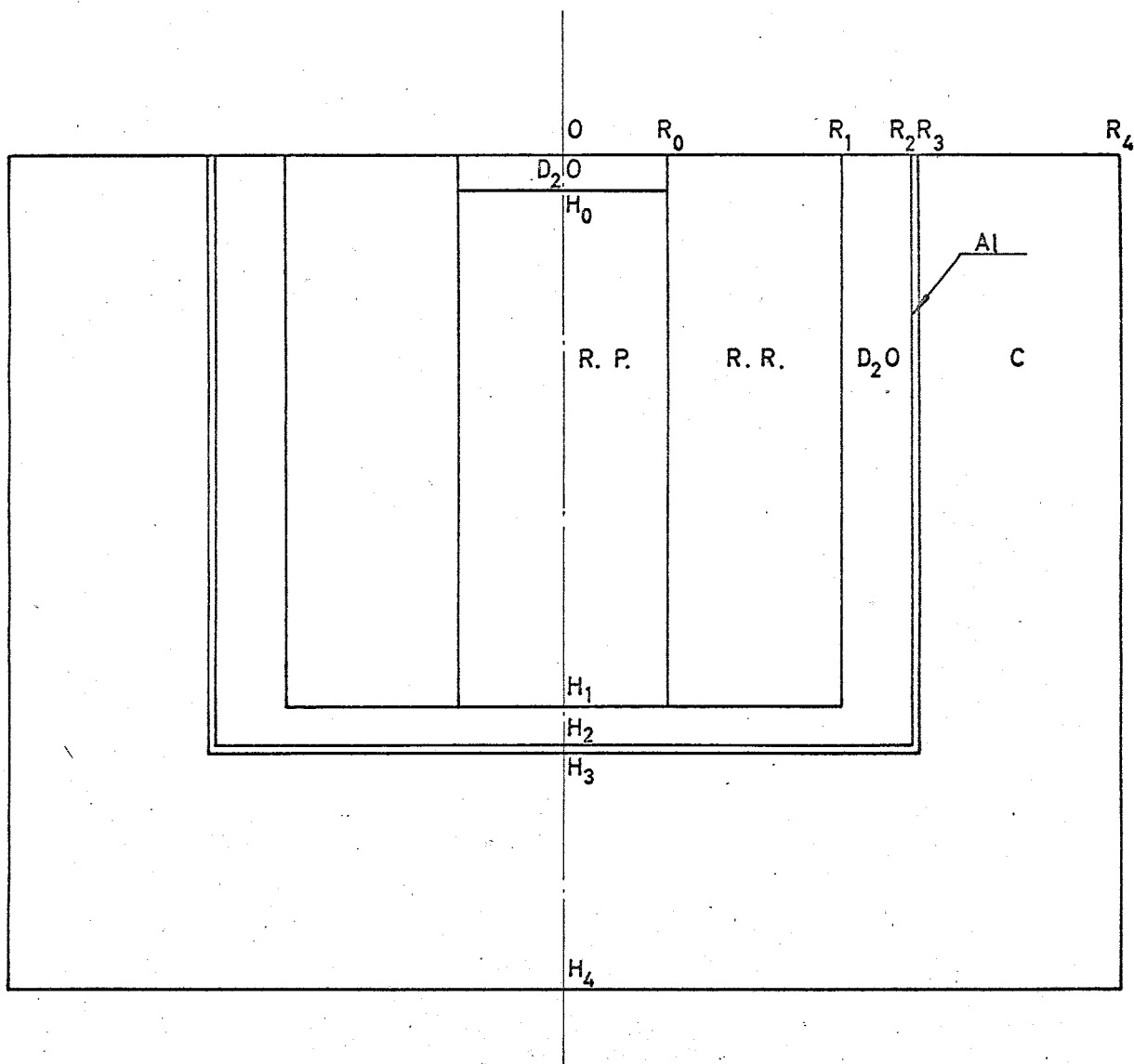


Fig. 4